

Rindler Observer Sublimation

J. A. Rosabal

*Center for theoretical physics of the universe, Institute for Basic Science,
55, Expo-ro, Yuseong-gu, Daejeon, Korea, 34126.*

In this note we discuss the sublimation of an object moving with proper constant acceleration, i.e., a Rindler observer. We focus on charged matter particles for the discussions but for simplicity we present the quantization of the neutrally charged massive scalar field in Rindler space. A non standard boundary conditions are used. We show that from them we get exactly the Bogoliubov coefficients we can get in the canonical quantization. The amplitude of emission and absorption by a Rindler observer, or accelerated detector, and its associated probability are computed in a novel fashion. We make a comparison between the Rindler observer sublimation and the black hole evaporation. We present three experimental setup, and we show that in two of them the probability of emission and absorption correspond to a thermal process. There is one situation, however, where deviations from thermality are found. It is numerically explored.

I. INTRODUCTION

Black hole evaporation [1–3] is perhaps the most amazing prediction in modern physics. However, its experimental confirmation is far from being reached. Mainly because of the probability of emission of a stellar black hole is ridiculously tiny. The life time, for instance, for a black hole of solar mass is much longer than the age of the universe [1]. This is an indication that this process is possible but unlikely. Despite this unlikeliness the efforts for understanding the phenomena related to the quantum mechanics of the black holes have not diminished over the years. Maybe because of the evaporation of these objects leads to the most shocking paradox in physics, the information paradox [4].

A related phenomenon which could offers some hints about the black hole quantum mechanics is the Unruh effect [5–7]. A Rindler observer, an object with proper constant acceleration (we will refer to it as accelerated detector too), experiences the vacuum as full of real pairs of entangled particle-antiparticle [8, 9] and hence it perceives thermal radiation.

It turns out that under certain considerations a particle with proper constant acceleration might evaporate too. We will consider the Rindler observers as solid objects, and the final state of its constituents as a gas, for instance, of electrons. This is why we will refer to this process as *Rindler observer sublimation*.

In this paper we will discuss the sublimation process of the accelerated detector. We shall consider the amplitudes and their associated probability of emission and absorption of matter particles by a Rindler observer. Here we focus on electrons and positrons. We shall also discuss the interpretation of the amplitudes and probabilities in correspondence to the experiment. We will show that there are three possible experimental setups where we can get quantitatively different results related to the thermal nature of the radiation.

Our results are presented in parallel to reference [3]. In the end we will conclude that the sublimation of a Rindler observer is not too different to the evaporation of a black

hole. Although, no information paradox appears in the case under consideration.

As we will show, and it is well known [7, 10], the probabilities of emission and absorption of the accelerated particle correspond to a thermal process. However, we will see how from the Minkowski observer point of view there could be situations where deviations from thermality can be found. This is an observation intrinsically connected to the uniformly accelerated particles which does not have any analog in black holes.

In [3] the Feynman worldline path integral (WPI) formulation [11, 12] was used to derive the propagator between two points in the black hole geometry. One point inside the horizon and the other outside. Two different coordinate patches are used to specify their location. In this work with the end of getting the amplitudes we will be interested in computing the propagator between one point in the Rindler coordinate patch and another point in the Minkowski coordinate patch. We will not use the WPI as our main tool to derive the Green's function, but supported by the WPI we will extract some useful information that will allow us to make conclusions on which propagator is the appropriate for obtaining the amplitudes.

The worldline path integral formulation offers an intuitive way of representing the emission and absorption processes. When focusing on electrons and positrons the quantum vacuum in the WPI formulation can be described in terms of loops.

A Rindler observer experiences the vacuum as full of real pairs of particle-antiparticle Fig 1, [8, 9]. They pop out from the vacuum in pairs and after some time they annihilate into it. Based on these two observations, in what follows we will elaborate the idea of *sublimation of an uniformly accelerated particle*.

Suppose that among the constituents of the accelerated detector there are electrons. When one of these electrons meet a positron in a pair created out form the vacuum, they annihilate each other, Fig 1, and one photon is emitted. After this interaction the remaining electron in the pair does not have an antiparticle to annihilate with anymore, and it goes free. In other words, the loop gets

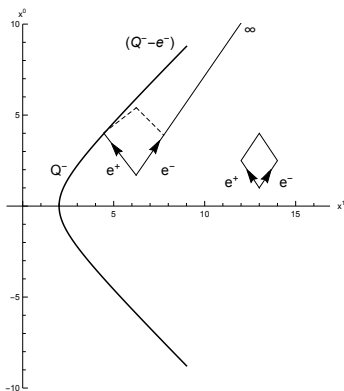


FIG. 1. Pictorial representation of the Rindler observer sublimation and the vacuum loops. The dashed lines represent the trajectories that the particles would have followed if the positron had not interacted with the Rindler observer. For simplicity we have omitted the photon emission.

broken by the detection. This free electron could be detected by a Minkowski observer. From the point of view of the accelerated detector a positron was absorbed from the vacuum. From the Minkowski observer perspective it looks like the accelerated detector emitted an electron.

If a Rindler observer emits a particle it would be perceived by a Minkowski observer as emission. In addition, if a Rindler observer absorbs an antiparticle from the vacuum it would be perceived as emission too by a Minkowski observer. An important observation from this picture is that while the Minkowski observer is detecting electrons the accelerated particle, either by emission or by absorption, is losing its constituents. This process is similar to the evaporation of a black hole.

The initial state in the process in Fig. 1 is the Minkowski vacuum $|0^M\rangle$. The final state, just before the detection by the accelerated detector, is a two particles state. One of these particles is regarded from the Rindler perspective while the other is from the Minkowski point of view. The process in question is

$$\left(\begin{array}{c} \text{Minkowski} \\ \text{vacuum} \end{array} \right) \longrightarrow \left(\begin{array}{c} \text{1-Rindler mode} \\ + \\ \text{1-Minkowski particle} \end{array} \right), \quad (1)$$

of course, in the presence of an uniformly accelerated object. When a Rindler mode is absorbed by the accelerated detector the final state in the field is $b_{(\nu, \bar{k})}^\dagger a_{(k'_1, \bar{k}')} |0^M\rangle$, but when it is emitted the resultant state is $b_{(\nu, \bar{k})}^\dagger a_{(k'_1, \bar{k}')} |0^M\rangle$. The amplitudes of detection of particles by the two observers can be easily obtained from

$$\begin{aligned} &\langle 0^M | a_{(k'_1, \bar{k}')} b_{(\nu, \bar{k})}^\dagger | 0^M \rangle \\ &\langle 0^M | a_{(k'_1, \bar{k}')} b_{(\nu, \bar{k})} | 0^M \rangle. \end{aligned} \quad (2)$$

By computing the amplitudes (2) we will find that this process is unlikely too. Although, there is an experimental setup where a small window for confirmation can be

found. We believe that because of this small window a similar attention to the one we pay to the black hole evaporation phenomenon should be paid to the Rindler observer sublimation. At the end of the day, we may never see a black hole evaporating but we could see an accelerated particle sublimating.

The paper is organized as follows. In section II the quantization in Rindler space using different boundary conditions to the ordinary ones in the canonical quantization is reviewed. The interpretation of (2) is discussed in section III. In this section a new derivation is presented in parallel to reference [3]. Three experimental situations are presented. In particular one of them leads to a non thermal emission. Strictly speaking, it could be called “a non thermal detection by the Minkowski observer,” this will be clarified in III A. The non thermal radiance is numerically explored in III B. After conclusions two appendixes are presented.

II. LAGRANGIAN QUANTIZATION

In this section we present the quantization of the massive scalar field in Rindler space following [8, 9]. For simplicity we will work with a massive neutrally charged scalar field, but this work can be easily extended to massive charged scalars or fermions.

In [8, 9] in contrast to the ordinary canonical quantization, the field operator is subjected to the boundary conditions

$$\begin{aligned} \varphi_R(\tau_i, \rho, \bar{x}) &= \varphi_M(x^0(\tau_i, \rho), x^1(\tau_i, \rho), \bar{x}), \\ \varphi_R(\tau_f, \rho, \bar{x}) &= \varphi_M(x^0(\tau_f, \rho), x^1(\tau_f, \rho), \bar{x}), \end{aligned} \quad (3)$$

where

$$\begin{aligned} x^0(\tau, \rho) &= \rho \sinh(\tau), \\ x^1(\tau, \rho) &= \rho \cosh(\tau). \end{aligned} \quad (4)$$

These are the boundary conditions that are consistent with the Lagrangian approach of field theory. In the Rindler frame φ_R , is specified at the initial and final time τ_i, τ_f , respectively. These are the slices that intersect the points where the acceleration is turned on and off. The operator φ_M , can be obtained in the canonical quantization in Minkowski space from the solution of

$$(\square - m^2)\varphi_M(x^0, x^1, \bar{x}) = 0. \quad (5)$$

The massive scalar field action in the Rindler wedge $\tau_i < \tau < \tau_f$ reads

$$\begin{aligned} S &= -\frac{1}{2} \int_{\tau_i}^{\tau_f} d\tau \int_0^\infty d\rho \int_{-\infty}^\infty d^2x \left[-\rho^{-1} (\partial_\tau \varphi_R)^2 \right. \\ &\quad \left. + \rho ((\partial_\rho \varphi_R)^2 + (\partial_{x^2} \varphi_R)^2 + (\partial_{x^3} \varphi_R)^2 + m^2 \varphi_R^2) \right]. \end{aligned} \quad (6)$$

The variation of (6) subjected to $\delta\varphi_R(\tau_i, \rho, \bar{x}) = \delta\varphi_R(\tau_f, \rho, \bar{x}) = 0$, and $\delta S = 0$, leads to

$$(\square - m^2)\varphi_R(\tau, \rho, \bar{x}) = 0. \quad (7)$$

The general solution of (5) is

$$\varphi_M(x^0, x^1, \bar{x}) = \int_{-\infty}^{\infty} \frac{dk_1}{2\pi} \int_{-\infty}^{\infty} \frac{d^2k}{(2\pi)^2} \frac{1}{(2k_0)^{\frac{1}{2}}} \left(a_{(k_1, \bar{k})} e^{-i(k_0 x^0 + k_1 x^1 + \bar{k} \cdot \bar{x})} + a_{(k_1, \bar{k})}^\dagger e^{i(k_0 x^0 + k_1 x^1 + \bar{k} \cdot \bar{x})} \right). \quad (8)$$

While the general solution of (7) reads [5]

$$\varphi_R(\tau, \rho, \bar{x}) = \int_0^{\infty} d\nu \int_{-\infty}^{\infty} \frac{d^2k}{(2\pi)^2} \frac{1}{(2\nu)^{\frac{1}{2}}} \left(b_{(\nu, -\bar{k})} e^{-i\nu\tau} + b_{(\nu, \bar{k})}^\dagger e^{i\nu\tau} \right) \psi_{\nu, \kappa}(\rho) e^{i\bar{k} \cdot \bar{x}}, \quad (9)$$

with

$$\kappa = (|\bar{k}|^2 + m^2)^{\frac{1}{2}}, \quad (10)$$

and

$$k_0 = (k_1^2 + |\bar{k}|^2 + m^2)^{\frac{1}{2}} = (k_1^2 + \kappa^2)^{\frac{1}{2}}, \quad (11)$$

$|\bar{k}|^2 = k_2^2 + k_3^2$, and $\psi_{\nu, \kappa}(\rho)$, the normalized eigenfunctions of the equation

$$\left(\rho^2 \frac{d^2}{d\rho^2} + \rho \frac{d}{d\rho} - \kappa^2 \rho^2 + \nu^2 \right) \psi_{\nu, \kappa}(\rho) = 0, \quad (12)$$

$$\psi_{\nu, \kappa}(\rho) = \pi^{-1} (2\nu \sinh(\pi\nu))^{\frac{1}{2}} K_{i\nu}(\kappa\rho), \quad (13)$$

$$\int_0^{\infty} \frac{d\rho}{\rho} \psi_{\nu, \kappa}(\rho) \psi_{\nu', \kappa}(\rho) = \delta(\nu - \nu'), \quad (14)$$

where $K_{i\nu}(\kappa\rho)$, are the modified Bessel function of the second kind.

Imposing (3) we get the equations

$$e^{-i\nu\tau_i} b_{(\nu, -\bar{k})} + e^{i\nu\tau_i} b_{(\nu, \bar{k})}^\dagger = (2\nu)^{\frac{1}{2}} \int_0^{\infty} d\rho \int_{-\infty}^{\infty} d^2x \frac{\psi_{\nu, \kappa}(\rho)}{\rho} e^{-i\bar{k} \cdot \bar{x}} \varphi_M(\tau_i, \rho, \bar{x}), \quad (15)$$

and

$$e^{-i\nu\tau_f} b_{(\nu, -\bar{k})} + e^{i\nu\tau_f} b_{(\nu, \bar{k})}^\dagger = (2\nu)^{\frac{1}{2}} \int_0^{\infty} d\rho \int_{-\infty}^{\infty} d^2x \frac{\psi_{\nu, \kappa}(\rho)}{\rho} e^{-i\bar{k} \cdot \bar{x}} \varphi_M(\tau_f, \rho, \bar{x}), \quad (16)$$

we have used the short hand notation

$$\varphi_M(\tau, \rho, \bar{x}) = \varphi_M(x^0(\tau, \rho), x^1(\tau, \rho), \bar{x}). \quad (17)$$

Solving for $b_{(\nu, \bar{k})}$, we get

$$b_{(\nu, \bar{k})} = -i \frac{(2\nu)^{\frac{1}{2}}}{2\sin[\nu(\tau_f - \tau_i)]} \int_0^{\infty} d\rho \int_{-\infty}^{\infty} d^2x \frac{\psi_{\nu, \kappa}(\rho)}{\rho} e^{i\bar{k} \cdot \bar{x}} \left[e^{i\nu\tau_f} \varphi_M(\tau_i, \rho, \bar{x}) - e^{i\nu\tau_i} \varphi_M(\tau_f, \rho, \bar{x}) \right]. \quad (18)$$

In [8, 9] an alternative way of deriving the vacuum energy was presented. It highlights the loops and the open paths contributions to the Rindler vacuum energy.

Here we shall present the Bogoliubov coefficients derived from the boundary conditions (3). It will be surprising for the reader, despite we are using different boundary conditions to (A1), form (3) we get exactly the Bogoliubov coefficients we can obtain from the canonical quantization [5], see Appendix A.

For this purpose we solve integrals of the form

$$\int_0^{\infty} d\rho \int_{-\infty}^{\infty} d^2x \frac{\psi_{\nu, \kappa}(\rho)}{\rho} e^{i\bar{k} \cdot \bar{x}} \varphi_M(\tau, \rho, \bar{x}), \quad (19)$$

which equals to

$$\frac{1}{4\pi\nu^{\frac{1}{2}}} \frac{1}{(\sinh(\pi\nu))^{\frac{1}{2}}} \int_{-\infty}^{\infty} d\tilde{z} \left(a_{(z, \bar{k})} [(i)^{-i\nu} e^{-i\nu(\tau+z)} + (i)^{i\nu} e^{i\nu(\tau+z)}] + a_{(z, -\bar{k})}^\dagger [(i)^{-i\nu} e^{i\nu(\tau+z)} + (i)^{i\nu} e^{-i\nu(\tau+z)}] \right), \quad (20)$$

where

$$z = \operatorname{arcsinh}\left(\frac{p_1}{\kappa}\right), \quad (21)$$

and

$$d\tilde{z} = \kappa^{\frac{1}{2}} (\cosh(z))^{\frac{1}{2}} dz = \frac{dp_1}{(\sqrt{p_1^2 + \kappa^2})^{\frac{1}{2}}}. \quad (22)$$

Plugging (20) in (18) we get

$$b_{(z, \bar{k})} = \frac{1}{2\pi} \frac{1}{(e^{2\pi\nu} - 1)^{\frac{1}{2}}} \int_{-\infty}^{\infty} d\tilde{z} \left(e^{\pi\nu} a_{(z, \bar{k})} + a_{(z, -\bar{k})}^\dagger \right) e^{-i\nu z}. \quad (23)$$

Using (21) and (22) we arrive at (A5) which are the Bogoliubov coefficients as presented, for instance, in [5]. We emphasize that here they have been obtained from (3).

The vacuum energy E_{vac}^R in Rindler space is given by

$$E_{vac}^R = \int_{-\infty}^{\infty} \frac{d^2k}{(2\pi)^2} \int_0^{\infty} d\nu \nu \langle 0^M | b_{(\nu, \bar{k})}^\dagger b_{(\nu, \bar{k})} | 0^M \rangle + E_0^R, \quad (24)$$

where

$$E_0^R = \frac{1}{2}\delta(0)^3 \int_{-\infty}^{\infty} d^2k \int_0^{\infty} d\nu\nu, \quad (25)$$

is the contribution of the loops inside the Rindler wedge, as discussed in [8]. Usually, this contribution is discarded. The Minkowski vacuum $|0^M\rangle$, satisfies $a_{(k_1, \bar{k})}|0^M\rangle = 0$. The thermal distribution can be easily computed using (A5) and (44),

$$E_{vac}^R = \int_{-\infty}^{\infty} \frac{d^2k}{(2\pi)^2} \int_0^{\infty} d\nu \frac{\nu}{e^{2\pi\nu} - 1} V_3 + E_0^R, \quad (26)$$

where

$$2\pi\delta(0) = \int_{-\infty}^{\infty} dx = V_1, \quad V_1^3 = V_3. \quad (27)$$

III. RINDLER OBSERVER SUBLIMATION

When the Unruh effect for matter particles is described in terms of worldline path integrals new and surprising features can be appreciated [8, 9]. We shall argue about the *sublimation of an uniformly accelerated particle*. Usually the Unruh effect is referred to electromagnetic fields (radiation). Nevertheless, when focusing on gauge fields only, there is not room for introducing the idea of sublimation.

As discussed in the introduction, supported by the WPI for matter particles a clear picture of sublimation arises. In fact this picture explains the controversial statement in [7] that we quote below.

What the detector regards as the detection (and thus absorption) of a Φ quantum, the Minkowski observer sees as the emission by the detector of such a quantum.

It seems contradicting that an observer regards a process as absorption while another observer regards the same process as emission. However, as described above, and depicted in Fig. 1, within the worldline path integral framework, when we regard the vacuum as a collection of loops, no contradiction arises.

The accelerated detector at some initial time can be idealized as a solid made of electrons (and other particles). After some time all these electrons would be part of the radiation, namely they could be considered as a gas of electrons. This is why we have chosen to call this process *Rindler observer sublimation*. How likely this process could be? We will answer this question by computing the probability of emission and absorption in the next section.

A. Amplitudes and Thermal Radiance

Let us now compute the amplitude associated to the detection of particles at the accelerated detector and by

a Minkowski observer. Namely, the amplitude for the process in Fig. 1. To achieve that it will be useful to know that if a Rindler mode is emitted by the accelerated detector, a Rindler mode is created in the Minkowski vacuum leading to the new state $b_{(\nu, \bar{k})}^\dagger|0^M\rangle$. Conversely, if a Rindler mode is absorbed by the accelerated detector, in the Minkowski vacuum a Rindler mode is annihilated leading to $b_{(\nu, \bar{k})}|0^M\rangle$.

Notice that we could have obtained the same amplitudes (2) considering the initial state as $b_{(\nu, \bar{k})}|0^M\rangle$, or $b_{(\nu, \bar{k})}^\dagger|0^M\rangle$, and the final state as $a_{(k'_1, \bar{k}')}^\dagger|0^M\rangle$. In the rest of the paper we will adopt this process i.e.,

$$\left(\begin{array}{c} \text{1-Rindler} \\ \text{mode} \end{array} \right) \longrightarrow \left(\begin{array}{c} \text{1-Minkowski} \\ \text{particle} \end{array} \right),$$

instead (1) just because it will be useful for the subsequent discussions.

The amplitude of detecting one particle from the Minkowski perspective associated to the emission or absorption by the accelerated particle can be computed by means of

$$A_{emi} = \langle 0^M | a_{(k'_1, \bar{k}')} b_{(\nu, \bar{k})}^\dagger | 0^M \rangle = \frac{e^{\pi\nu}}{(e^{2\pi\nu} - 1)^{\frac{1}{2}}} \frac{1}{\sqrt{k'_0}} \left(\frac{k'_0 + k'_1}{k'_0 - k'_1} \right)^{\frac{1}{2}i\nu} (2\pi)^2 \delta^2(\bar{k}' - \bar{k}), \quad (28)$$

or

$$A_{abs} = \langle 0^M | a_{(k'_1, \bar{k}')} b_{(\nu, \bar{k})} | 0^M \rangle = \frac{1}{(e^{2\pi\nu} - 1)^{\frac{1}{2}}} \frac{1}{\sqrt{k'_0}} \left(\frac{k'_0 + k'_1}{k'_0 - k'_1} \right)^{-\frac{1}{2}i\nu} (2\pi)^2 \delta^2(\bar{k}' - \bar{k}), \quad (29)$$

where $k_0 = (k_1'^2 + |\bar{k}'|^2 + m^2)$. Here we have used (A5).

The total probability will be the sum over all initial modes [3] of the square of the amplitude. A Rindler mode is fully specified by three number (ν, k_2, k_3) . For a definite frequency mode the total amplitude is

$$P_{emi} = \int_{-\infty}^{\infty} \frac{d^2\bar{k}}{(2\pi)^2} \frac{|A_{emi}|^2}{V_2},$$

$$P_{abs} = \int_{-\infty}^{\infty} \frac{d^2\bar{k}}{(2\pi)^2} \frac{|A_{abs}|^2}{V_2}. \quad (30)$$

The formal square of the δ function is considered as

$$\delta^2(\bar{k}' - \bar{k}) = \frac{V_2}{(2\pi)^2} \delta(\bar{k}' - \bar{k}), \quad (31)$$

where we have used (27). One can avoid these formal manipulations using wave packets, see for instance [13].

Notice that the total probabilities fulfil the relation [3, 10]

$$\frac{P_{abs}}{P_{emi}} = e^{-2\pi\nu}, \quad (32)$$

which indicates that the emission and absorption process is thermal with a temperature

$$T = \frac{\hbar \mathbf{a}}{2\pi c k_B}, \quad (33)$$

we have restored the acceleration \mathbf{a} and the physical constants.

We want to make a parenthesis here to discuss what transition amplitudes we are computing in (28) and (29). The final Minkowski state involved in (28) and (29) is defined over a space-like slice at the Minkowski time $x^0 = +\infty$. So, it means that if we wait long enough there will be transitions from Rindler modes to Minkowski modes, and perhaps we (Minkowski observers in our lab) will be able to detect particles coming out from the Rindler observer. However, (28) and (29) do not tell us how and where to measure in the three dimensional space in order to detect these particles.

In what follows we present a different derivation of the radiance of a Rindler observer. In this it will be clear how and where we should look at in order to detect some radiated particles. This calculation will be made in analogy to the one presented in [3] for the black hole radiance. It will show that the radiative processes of a Rindler observer are no so different to the same processes in a black hole. In the end we will conclude that in the same way a black hole evaporates [3] a Rindler observer sublimates.

As we are dealing with the emission and absorption of one particle we can use the probability current

$$J_\mu(x) = -i(\varphi_2^*(x)\partial_{x^\mu}\varphi(x) - \partial_{x^\mu}\varphi_2^*(x)\varphi(x)), \quad (34)$$

to compute the amplitude. By proceeding in this way we will gain some intuition about how to detect the radiated particles.

First, suppose we place a screen which will be our particle detector (Minkowski observer or detector) perpendicular to the direction of motion of the accelerated observer, as indicated in Fig. 2. This detector measures on shell $k_0^2 = k_1^2 + |\vec{k}|^2 + m^2$, purely positive energy particles in modes $\varphi_2(x)$. The location of the screen will be specified through the calculation. We will consider three situations. The screen placed to the left/right of $x^1 = \rho_1$, and $R \rightarrow +\infty$.

The amplitude of detecting a mode $\varphi_2(x)$, at the screen $x^1 = R$, from the Minkowski perspective, having started at $\rho = \rho_1$, in a mode $\varphi_1(y)$, from the Rindler perspective is

$$A = \int_{\text{screen}} J_\mu(x)n^\mu = \int_{-\infty}^{\infty} dx^0 \int_{-\infty}^{\infty} d^2\vec{x} J_1(x)n^1 \Big|_{x^1=R}, \quad (35)$$

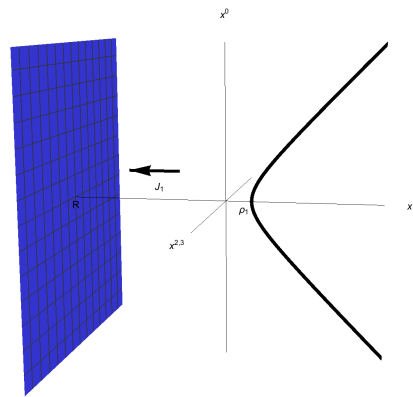


FIG. 2. Pictorial representation in spacetime of the experimental setup. In blue the screen (Minkowski detector). The thick black line represents the Rindler detector. In this setup the screen is placed to the left of $x^1 = \rho_1$. J_1 , represents the current associated to an incoming wave moving from right to left.

where

$$\varphi(x) = \rho_1 \int_{-\infty}^{\infty} d\tau \int_{-\infty}^{\infty} d^2\vec{y} \left(\varphi_1(y)\partial_\rho G(x,y) - G(x,y)\partial_\rho\varphi_1(y) \right) \Big|_{\rho=\rho_1}, \quad (36)$$

and $n^\mu = (0, 1, 0, 0)$, is the normal vector to the screen. Here the coordinates x are referred to the Minkowski observer, $x = (x^0, x^1, \vec{x})$, while $y = (\tau, \rho, \vec{y})$, are the Rindler coordinates. The appearance of ρ_1 in front of the integral (36) is due to the volume measure on the surface $\rho = \rho_1$, i.e., $ds^2 = -\rho^2 d\tau^2 + d\rho^2 + d\vec{y}^2$, hence $\sqrt{-h}|_{\rho=\rho_1} d\tau d^2\vec{y} = \rho_1 d\tau d^2\vec{y}$. The Green's function $G(x, y)$, has one of its entry evaluated only at the Rindler coordinate patch.

The question at this point is what Green's function should we use in (36) since one point is in the Rindler coordinate patch and the other point is in the Minkowski coordinate patch. To answer it we can proceed as in [3]. In this reference, one of the point where the Green's function is evaluated resides inside the horizon while the other point belongs to the exterior part.

For deriving the Green's function between two points (no matter the location of these points) we can use its worldline path integral representation

$$G(x, y) = \int_0^\infty ds e^{-\frac{1}{2}im^2s} \int_{x(0)=y}^{x(1)=x} Dx^\mu(\tau) \exp \left[i \frac{1}{4s} \int_0^1 d\tau \dot{x}^2(\tau) \right]. \quad (37)$$

The point x belongs to the Minkowski coordinate patch. The point y belongs to the Rindler coordinate patch, but

the wedge is just a part of Minkowski space. So, we can regard y as belonging to Minkowski space. With this in mind, the path integration in (37) should be over all the path starting at y and ending at x in the Minkowski space. The derivation of $G(x, y)$ from (37) is a well known calculation, see for instance [11, 12], and it leads to

$$G(x, y) = \int_{-\infty}^{\infty} \frac{d^4 p}{(2\pi)^4} \frac{e^{-i((x^0-y^0)k_0+(x^1-y^1)k_1+(\bar{x}-\bar{y})\cdot\bar{k})}}{p^2 - m^2 + i\epsilon}, \quad (38)$$

with y restricted to the right wedge, i.e.,

$$\begin{aligned} y^0 &= \rho \sinh(\tau), \\ y^1 &= \rho \cosh(\tau). \end{aligned} \quad (39)$$

Relations (34), (35) and (36) can be combined in a more compact form

$$A = - \int d\sigma^\mu(x) \int d\sigma^\nu(y) \varphi_2^*(x) \overleftrightarrow{\partial}_\mu G(x, y) \overleftrightarrow{\partial}_\nu \varphi_1(y), \quad (40)$$

where the integral over x is taken over the surface $x^1 = R$, and the integral over y is over the surface $\rho = \rho_1$, and $a \overleftrightarrow{\partial}_\mu b = a \partial_\mu b - b \partial_\mu a$. This formula is similar to (4.1) of reference [3] in the case of a black hole.

In order to proceed we need to find $\varphi_1(y)$, and $\varphi_2(x)$. They are the quantum mechanical wave functions. To be consistent with our conventions we will use the mode expansion (9) together with (A5) to compute the wave functions. The emission wave function from the Rindler point of view is given by

$$\begin{aligned} \varphi_1(y) &= \langle 0^M | \varphi_R(\tau, \rho, \bar{y}) b_{(\nu, \bar{k})}^\dagger | 0^M \rangle \\ &= N_1 e^{-i\nu\tau} K_{i\nu}(\kappa\rho) e^{-i\bar{k}\cdot\bar{y}}, \end{aligned} \quad (41)$$

where $N_1 = \frac{1}{\sqrt{2\pi}} \frac{e^{\frac{3}{2}\pi\nu}}{(e^{2\pi\nu}-1)^{\frac{1}{2}}}$. On the other hand the absorption wave function is

$$\begin{aligned} \varphi_1(y) &= \langle 0^M | \varphi_R(\tau, \rho, \bar{y}) b_{(\nu, \bar{k})} | 0^M \rangle \\ &= N'_1 e^{i\nu\tau} K_{i\nu}(\kappa\rho) e^{i\bar{k}\cdot\bar{y}}, \end{aligned} \quad (42)$$

where $N'_1 = \frac{1}{\sqrt{2\pi}} \frac{e^{-\frac{1}{2}\pi\nu}}{(e^{2\pi\nu}-1)^{\frac{1}{2}}}$. Notice that they have support only in the right Rindler wedge. Finally, the Minkowski wave function is simple given by

$$\begin{aligned} \varphi_2(x) &= \langle 0^M | \varphi_M(x) a_{(k_1, \bar{k})}^\dagger | 0^M \rangle \\ &= \frac{1}{\sqrt{2k_0}} e^{-ikx} = N_2 e^{-ikx}. \end{aligned} \quad (43)$$

We have used the relation

$$\int_{-\infty}^{\infty} \frac{dp_1}{p_0} \left(\frac{p_0 + p_1}{p_0 - p_1} \right)^{\frac{1}{2}i(\nu' - \nu)} = (2\pi) \delta(\nu' - \nu), \quad (44)$$

which can be easily proved by the change of variable $z = \frac{1}{2} \text{Log} \left(\frac{p_0 + p_1}{p_0 - p_1} \right)$. Although the Rindler wave functions have

support only on the right wedge they can be written as localized (inside Rindler space) Minkowski wave package (B5) and (B6).

Let us present the calculation of the emission amplitude. For this we use (41) and (43). After some algebra from (40) one arrives at

$$\begin{aligned} A_{emi} &= \frac{1}{2} N_1 N_2 \rho_1 e^{ik_1^{(2)} R} (2\pi)^2 \delta^2(\bar{k}^{(2)} - \bar{k}^{(1)}) \\ &\quad \left(K_{i\nu}(\kappa\rho_1) \partial_\rho - \partial_\rho K_{i\nu}(\kappa\rho_1) \right) \left(\partial_{x^1} - ik_1^{(2)} \right) \\ &\quad \int_{-\infty}^{\infty} d\tau \frac{e^{-i|x^1-y^1||k_1^{(2)}|}}{|k_1^{(2)}|} e^{ik_0^{(2)} y^0 - i\nu\tau} \Big|_{\substack{\rho = \rho_1 \\ x^1 = R}}, \end{aligned} \quad (45)$$

recall that y^0 and y^1 are given in (39).

We shall consider first the case depicted in Fig. 2, i.e., $x^1 = R < \rho_1$, which implies that $x^1 - y^1 = R - \rho_1 \cosh(\tau) < 0$, for all τ , and an incoming wave moving from right to left with $k_1^{(2)} < 0$. Under these considerations (45) reduces to

$$\begin{aligned} A_{emi} &= i N_1 N_2 \rho_1 (2\pi)^2 \delta^2(\bar{k}^{(2)} - \bar{k}^{(1)}) \\ &\quad \left(K_{i\nu}(\kappa\rho_1) \partial_\rho - \partial_\rho K_{i\nu}(\kappa\rho_1) \right) \\ &\quad \int_{-\infty}^{\infty} d\tau e^{ik_1^{(2)} y^1 + ik_0^{(2)} y^0 - i\nu\tau} \Big|_{\rho = \rho_1}, \end{aligned} \quad (46)$$

where no R dependence appears. Being careful we can analytically extend the previous integral, see Appendix B, to get

$$\begin{aligned} A_{emi} &= \frac{1}{2} i N_1 N_2 \rho_1 (2\pi)^2 \pi^2 \delta^2(\bar{k}^{(2)} - \bar{k}^{(1)}) \\ &\quad e^{-\frac{1}{2}\pi\nu} \left(\frac{k_0^{(2)} + k_1^{(2)}}{k_0^{(2)} - k_1^{(2)}} \right)^{\frac{1}{2}i\nu} \\ &\quad \left(H_{i\nu}^{(1)}(i\kappa\rho_1) \partial_\rho H_{i\nu}^{(2)}(i\kappa\rho_1) - \partial_\rho H_{i\nu}^{(1)}(i\kappa\rho_1) H_{i\nu}^{(2)}(i\kappa\rho_1) \right), \end{aligned} \quad (47)$$

where $H_{i\nu}^{(a)}(z)$, $a = 1, 2$, are the Hankel functions, and we have used the relation (B7). Notice that the expression in the last parenthesis of (47) is the Wronskian involving the Hankel functions. It equals to

$$-\frac{4i}{\pi\rho_1}. \quad (48)$$

Plugging (48) in (47) we see that ρ_1 cancels out and after a few steps we get (28). Proceeding in the same way for the absorption amplitude we can obtain similar results.

We have computed the emission amplitude using the flux of probabilities and we have got the expected result (28) and (29). So far there are no experimental advantages in this calculation. Detecting the flux of particles is almost impossible since the temperature is extremely low

(33) for the reachable accelerations in the lab. Although, now we have a better picture on how and where we could detect radiated particles.

As we can see, under our considerations these amplitudes are independent of R and ρ_1 as long as the screen is placed to the left of ρ_1 . So, this could be placed as close as we wish from $x^1 = \rho_1$, to the left, and still detecting the radiated particles would be a difficult task.

Another experimental option we have would be to place the screen as depicted in Fig. 3. Notice that in this case there could be detection inside the right Rindler wedge and in both faces of the screen. The amplitudes

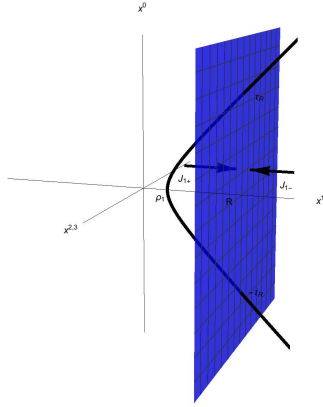


FIG. 3. Pictorial representation in spacetime of the experimental setup. In blue screen (Minkowski detector). The thick black line represents the Rindler detector. In this setup the screen is placed to the right of $x^1 = \rho_1$. J_{1-} , and J_{1+} , represent the current associated to the incoming waves in each side of the screen. τ_R , is the Rindler time where the accelerated particle meets the screen

for this case have a different behaviour. This is mainly because of now the accelerated particle intersects the screen. For instance, the left face perceives the process of emission and absorption of the accelerated detector happening in a finite time.

Let us sketch this calculation. Suppose that we prepare the particle detector in such a way that there is not interference of the incoming waves with opposite momentum at the screen. We find it convenient to work under this assumption because of we can treat left and right moving modes and amplitudes independently.

The amplitudes of detecting particles at the screen associated to the emission by a Rindler observer are

$$A_{emi-} = \int_{-\infty}^{\infty} dx^0 \int_{-\infty}^{\infty} d^2\bar{x} J_{1-}(x)$$

$$A_{emi+} = \int_{-\infty}^{\infty} dx^0 \int_{-\infty}^{\infty} d^2\bar{x} J_{1+}(x)$$

where the subscripts \pm indicate the direction of the incoming wave Fig. 3. Under similar considerations as in

our previous calculation, using (45), we get

$$A_{emi-} = iN_1 N_2 \rho_1 (2\pi)^2 \delta^2(\bar{k}^{(2)} - \bar{k}^{(1)}) \left(K_{i\nu}(\kappa\rho_1) \partial_\rho - \partial_\rho K_{i\nu}(\kappa\rho_1) \right) \left(\int_{-\infty}^{-\tau_R} d\tau + \int_{\tau_R}^{\infty} d\tau \right) e^{ik_1^{(2)} y^1 + ik_0^{(2)} y^0 - i\nu\tau} \Big|_{\rho=\rho_1}, \quad (49)$$

with $k_1^{(2)} < 0$, and

$$A_{emi+} = -iN_1 N_2 \rho_1 (2\pi)^2 \delta^2(\bar{k}^{(2)} - \bar{k}^{(1)}) \left(K_{i\nu}(\kappa\rho_1) \partial_\rho - \partial_\rho K_{i\nu}(\kappa\rho_1) \right) \int_{-\tau_R}^{\tau_R} d\tau e^{ik_1^{(2)} y^1 + ik_0^{(2)} y^0 - i\nu\tau} \Big|_{\rho=\rho_1}, \quad (50)$$

with $k_1^{(2)} > 0$, where τ_R , is the time where the accelerated particle meets the screen, $\tau_R = \text{arccosh}(\frac{R}{\rho_1})$. Notice that none combination of the integrals in (49) and (50) reproduces (46). We also have similar results for the absorption amplitudes.

From this calculation we can conclude that when the screen is placed to the right of $x^1 = \rho_1$, Fig. 3 we can find deviation from the thermal behaviour. From the Minkowski perspective, the thermal character of the radiation depends upon where it is collected. This is why we mentioned earlier that, strictly speaking, it could be called ‘‘a non thermal detection.’’

Let us now briefly present the third experimental option, the screen placed at $R \rightarrow \infty$. This limit can be taken on expressions (49) and (50). When $R \rightarrow \infty$, $\tau_R \rightarrow \infty$. The two integrals of (49) vanish, while (50) coincides with (46) and hence (28). So, when the screen is placed at $R \rightarrow \infty$ we recover the thermal behaviour.

One important feature of (46) is that the integral involved needs regularization, see Appendix B. However, the integral (50) can be highly oscillating but for finite τ_R , it will be finite. Taking this into consideration in next subsection we shall numerically explore the amplitudes A_{emi+} , and A_{abs+} , and their associated probabilities.

Experimentally having only A_{emi+} , and A_{abs+} could be achieved by blocking the right face of the screen in such a way that there is not detection on that side. Could this deviation from thermality open a window for detecting more easily the radiated particles? This is a question whose answer can be found in the next section.

B. Non thermal Radiance

The emission amplitude of detecting the incoming flux related to $J_{1+}(x)$, only, Fig. 3, is given by (50). Similarly for A_{abs+} . The probability of detection follows the same rules as in (30).

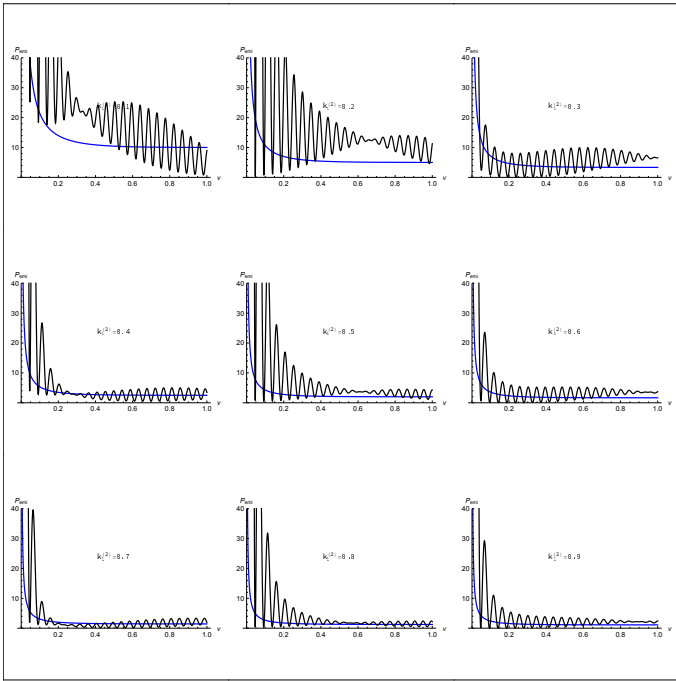


FIG. 4. Probability of detection associated to the emission. In blue the thermal probability. In black the non thermal probability. $R = 10$ and $\rho_1 = 1$.

Lest us first present the plot for different values of $k_1^{(2)}$, with $k_2^{(2)} = k_3^{(2)} = 0$, of the probability of detection from the Minkowski perspective, associated to the emission and absorption of a Rindler mode by the accelerated particle Fig. 4 and Fig. 5. The probability takes its maximum value when $k_2^{(2)} = k_3^{(2)} = 0$. For $k_2^{(2)} \neq 0$, and $k_3^{(2)} \neq 0$, the amplitude rapidly falls to zero.

From Fig. 4 and Fig. 5 we can see the oscillatory behaviour of the non thermal probabilities. We have used natural units $\hbar = c = k_B = \mathbf{a} = 1$. By restoring the constants we see that the probability is still insignificant. What is remarkable is that for certain values of the frequency ν the non thermal probability of detection (by the Minkowski observer) is greater than the thermal. Perhaps in this setup we could enhance the probability of detection by considering several accelerated particles, i.e., several Rindler and Minkowski modes in the initial and final state respectively.

We are referring to this result as “non thermal” however, so far we do not really know whether it is associated to a thermal process. A good test to diagnose the thermal nature of a given process comes from the ratio $\frac{P_{abs}}{P_{emi}}$.

In Fig. 6 we present a comparison between the ratio $\frac{P_{abs}}{P_{emi}} = e^{-2\pi\nu}$ for a thermal detection and the same ratio but related only to $J_{1+}(x)$.

From Fig. 6 we can clearly see that from the Minkowski perspective, under the conditions of the experiment, the process looks completely non thermal. For this case we can not associated a temperature to this radiation.

For the sake of completeness we present the plot of

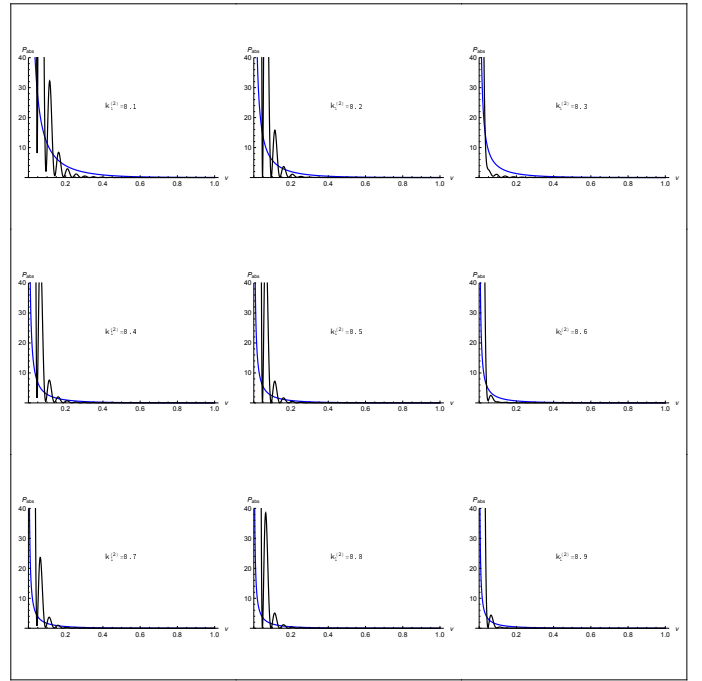


FIG. 5. Probability of detection associated to the absorption. In blue the thermal probability. In black the non thermal probability. $R = 10$ and $\rho_1 = 1$.

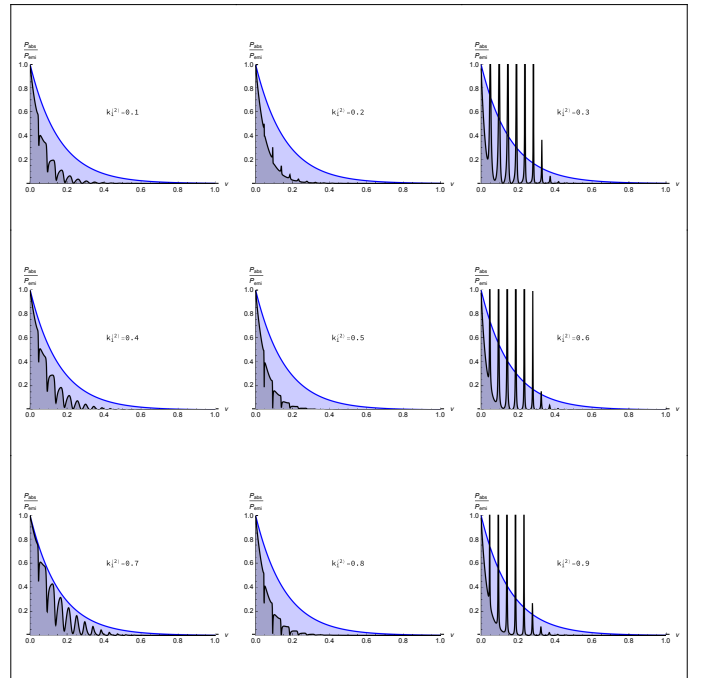


FIG. 6. Ratio between the probabilities associated to emission and absorption. In blue the thermal ratio. In black the non thermal ratio. $R = 10$ and $\rho_1 = 1$.

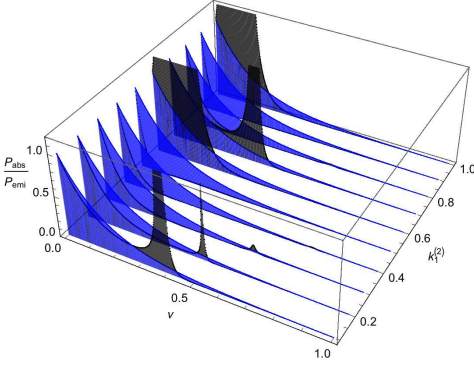


FIG. 7. Ratio between the probabilities associated to emission and absorption. In blue the thermal ratio. In black the non thermal ratio. $R = 10$, $\rho_1 = 1$ and $(k_2^{(2)})^2 + (k_3^{(2)})^2 = 0.6$.

the ratio between the probabilities when $k_2^{(2)} \neq 0$, and $k_3^{(2)} \neq 0$ in Fig. 7. We do not present the probabilities associated to it because they are difficult to appreciate in the figure.

From 7 we can see that for the intervals we are considering for the momentum $k_1^{(2)}$ and the frequency ν there are values where we can find huge deviations from the thermal behaviour.

ACKNOWLEDGMENTS

I am grateful to H. Casini, Pablo Diaz and Kanghoon Lee for discussions and useful comments. I would like specially thank Pablo Diaz who participated in the first steps of this research.

Appendix A: Bogoliubov coefficients, canonical quantization

In the canonical quantization in Rindler space instead of imposing the boundary condition (3) we impose

$$\begin{aligned} \varphi_R(\tau, \rho, \bar{x}) &= \varphi_M(x^0(\tau, \rho), x^1(\tau, \rho), \bar{x}), \\ \partial_\tau \varphi_R(\tau, \rho, \bar{x}) &= \partial_\tau \varphi_M(x^0(\tau, \rho), x^1(\tau, \rho), \bar{x}), \end{aligned} \quad (\text{A1})$$

at some initial Rindler time τ .

In this case we have the equations

$$\begin{aligned} e^{-i\nu\tau} b_{(\nu, -\bar{k})} + e^{i\nu\tau} b_{(\nu, \bar{k})}^\dagger &= \\ (2\nu)^{\frac{1}{2}} \int_0^\infty d\rho \int_{-\infty}^\infty d^2x \frac{\psi_{\nu, \kappa}(\rho)}{\rho} e^{-i\bar{k} \cdot \bar{x}} \varphi_M(\tau, \rho, \bar{x}), \end{aligned} \quad (\text{A2})$$

and

$$\begin{aligned} e^{-i\nu\tau} b_{(\nu, -\bar{k})} - e^{i\nu\tau} b_{(\nu, \bar{k})}^\dagger &= \\ i \frac{(2\nu)^{\frac{1}{2}}}{\nu} \int_0^\infty d\rho \int_{-\infty}^\infty d^2x \frac{\psi_{\nu, \kappa}(\rho)}{\rho} e^{-i\bar{k} \cdot \bar{x}} \partial_\tau \varphi_M(\tau, \rho, \bar{x}). \end{aligned} \quad (\text{A3})$$

Solving for $b_{(\nu, \bar{k})}$, we get

$$\begin{aligned} b_{(\nu, \bar{k})} &= \frac{1}{2} e^{i\nu\tau} (2\nu)^{\frac{1}{2}} \left(1 + \frac{i}{\nu} \partial_\tau \right) \\ &\int_0^\infty d\rho \int_{-\infty}^\infty d^2x \frac{\psi_{\nu, \kappa}(\rho)}{\rho} e^{i\bar{k} \cdot \bar{x}} \varphi_M(\tau, \rho, \bar{x}). \end{aligned} \quad (\text{A4})$$

Now we can use the result (20) in equation (A4) to finally obtain (23). We stress that the boundary conditions in the canonical quantization are different to the ones used in section II, but certainly they are equivalent. Using (21) and (22), (23) can be written as

$$\begin{aligned} b_{(\nu, \bar{k})} &= \frac{1}{2\pi} \frac{1}{(e^{2\pi\nu} - 1)^{\frac{1}{2}}} \int_{-\infty}^\infty \frac{dp_1}{\sqrt{p_0}} \left(\frac{p_0 + p_1}{p_0 - p_1} \right)^{-\frac{1}{2}i\nu} \\ &\times \left(e^{\pi\nu} a_{(p_1, \bar{k})} + a_{(p_1, -\bar{k})}^\dagger \right), \end{aligned} \quad (\text{A5})$$

where $p_0 = \sqrt{p_1^2 + \kappa^2}$, (10).

Appendix B: Integral representation of the Hankel functions

The integral representation of the Hankel functions can be found in [14]. Here we present the integral representation of $H_\nu^{(2)}((z^2 - \zeta^2)^{\frac{1}{2}})$, in connection with the Amplitude calculation and the wave function in the Rindler wedge.

This function can be represented as

$$\begin{aligned} H_\nu^{(2)}((z^2 - \zeta^2)^{\frac{1}{2}}) &= -\frac{1}{\pi i} e^{\frac{1}{2}\nu\pi i} \left(\frac{z + \zeta}{z - \zeta} \right)^{-\frac{1}{2}\nu} \\ &\int_{-\infty}^\infty d\tau e^{-iz\cosh(\tau) - i\zeta\sinh(\tau) - \nu\tau}, \end{aligned} \quad (\text{B1})$$

where $\nu, z, \zeta \in \mathbb{C}$, and $\text{Im}(z \pm \zeta) < 0$.

The integral in (46) can be rewritten as

$$\int_{-\infty}^\infty d\tau e^{-i(-k_1^{(2)}\rho)\cosh(\tau) - i(-k_0^{(2)}\rho)\sinh(\tau) - i\nu\tau}. \quad (\text{B2})$$

Now, the analytical extension of (B2) is defined as

$$(-i\pi) e^{\frac{1}{2}\nu\pi} \left(\frac{k_1^{(2)} + k_0^{(2)}}{k_1^{(2)} - k_0^{(2)}} \right)^{\frac{1}{2}i\nu} H_{i\nu}^{(2)} \left(\rho \sqrt{(k_1^{(2)})^2 - (k_0^{(2)})^2} \right). \quad (\text{B3})$$

The on shell condition $(k_0^{(2)})^2 - (k_1^{(2)})^2 - \kappa^2 = 0$ reduces the integral (B2) to

$$(-i\pi) e^{\frac{1}{2}\nu\pi} \left(\frac{k_1^{(2)} + k_0^{(2)}}{k_1^{(2)} - k_0^{(2)}} \right)^{\frac{1}{2}i\nu} H_{i\nu}^{(2)}(i\kappa\rho), \quad (\text{B4})$$

which is the result we have used in (47).

We can also use the integral representation of the Hankel function to relate the one particle wave functions (41) and (42) in Rindler space with a wave package in Minkowski space. They are related as: for the emission wave function

$$e^{-i\nu\tau}K_{i\nu}(\kappa\rho) = \frac{1}{2}e^{-\frac{1}{2}\nu\pi} \int_{-\infty}^{\infty} \frac{dk_1}{k_0} \left(\frac{k_0+k_1}{k_0-k_1}\right)^{\frac{1}{2}i\nu} e^{-i(k_0x^0+k_1x^1)}, \quad (\text{B5})$$

for the absorption wave function

$$e^{i\nu\tau}K_{i\nu}(\kappa\rho) = \frac{1}{2}e^{\frac{1}{2}\nu\pi} \int_{-\infty}^{\infty} \frac{dk_1}{k_0} \left(\frac{k_0+k_1}{k_0-k_1}\right)^{-\frac{1}{2}i\nu} e^{i(k_0x^0+k_1x^1)}. \quad (\text{B6})$$

Here we have followed three steps. First, we have performed the change of variables

$$\tau = \frac{1}{2}\text{Log}\left(\frac{x^1+x^0}{x^1-x^0}\right),$$

$$\rho = \sqrt{(x^1)^2 - (x^0)^2},$$

which is the inverse transformation of (4). Second, we have used the relation

$$K_{i\nu}(z) = \frac{\pi}{2}(i)^{i\nu+1}H_{i\nu}^{(1)}(iz), \quad (\text{B7})$$

and the integral representation of $H_{i\nu}^{(1)}(iz)$, see [14]. Finally, the change of variables

$$k_0 = \kappa \cosh(t),$$

$$k_1 = \kappa \sinh(t),$$

brings the wave functions to the desired form.

It is worth to emphasize that (B5) and (B6) hold only on the overlap between Rindler and Minkowski space. With this we can conclude that the Rindler one particle wave function can be seen as a fully localized (inside the Rindler wedge) wave package from the Minkowski perspective.

-
- [1] S. W. Hawking, *Nature* **248**, 30 (1974).
[2] S. W. Hawking, *Commun. Math. Phys.* **43**, 199 (1975)
Erratum: [*Commun. Math. Phys.* **46**, 206 (1976)].
[3] J. B. Hartle and S. W. Hawking, *Phys. Rev. D* **13**, 2188 (1976).
[4] S. W. Hawking, *Phys. Rev. D* **14**, 2460 (1976).
[5] S. A. Fulling, *Phys. Rev. D* **7**, 2850 (1973).
[6] P. C. W. Davies, *J. Phys. A* **8**, 609 (1975).
[7] W. G. Unruh, *Phys. Rev. D* **14**, 870 (1976).
[8] J. A. Rosabal, *Phys. Rev. D* **98**, no. 5, 056015 (2018).
[9] J. A. Rosabal, arXiv:1810.05523.
[10] I. Agullo, J. Navarro-Salas, G. J. Olmo and L. Parker, *New J. Phys.* **12**, 095017 (2010).
[11] R. P. Feynman, *Phys. Rev.* **80**, 440 (1950).
[12] M. J. Strassler, *Nucl. Phys. B* **385**, 145 (1992).
[13] John R. Taylor. "Scattering Theory: The Quantum Theory of Nonrelativistic Collisions." John Wiley and Sons, Inc., New York (1972).
[14] NIST Digital Library of Mathematical Functions. <http://dlmf.nist.gov/10.9>, Release 1.0.15. F.W.J. Olver, A.B. Olde Daalhuis, D.W. Lozier, B.I. Schneider, R.F. Boisvert, C.W. Clark, B.R. Miller, and B.V. Saunders, eds.